Eur. Phys. J. Special Topics **164**, 45–53 (2008)

DOI: 10.1140/epjst/e2008-00833-5

THE EUROPEAN PHYSICAL JOURNAL
SPECIAL TOPICS

Selection of recurrence threshold for signal detection

S. Schinkel[1,a], O. Dimigen[2], and N. Marwan[1,3]

[1] Interdisciplinary Centre for Dynamics of Complex Systems, University of Potsdam, 14415 Potsdam, Germany
[2] Department of Psychology, University of Potsdam, 14415 Potsdam, Germany
[3] Potsdam Institute for Climate Impact Research (PIK), 14412 Potsdam, Germany

Abstract. Over the last years *recurrence plots* (RPs) and *recurrence quantification analysis* (RQA) have become quite popular in various branches of science. One key problem in applying RPs and RQA is the selection of suitable parameters for the data under investigation. Whereas various well-established methods for the selection of embedding parameters exists, the question of choosing an appropriate threshold has not yet been answered satisfactorily. The recommendations found in the literature are rather rules of thumb than actual guidelines. In this paper we address the issue of threshold selection in RP/RQA. The core criterion for choosing a threshold is the power in signal detection that threshold yields. We will validate our approach by applying it to model as well as real-life data.

1 Introduction

As *recurrence plots* (RPs) and their quantification (*recurrence quantification analysis*, RQA) [11] are becoming ever more popular in many disciplines, beginners are often faced with the problem of finding suitable parameters for embedding and recurrence threshold. For finding suitable embedding parameters, different approaches were suggested, like auto-correlation, mutual information, false nearest neighbours etc., and were already discussed in the literature [2,4,6,19]. Yet the choice of the neighbourhood size is still under discussion and often causes uncertainties in applying RPs and RQA.

Several rules of thumb for the choice of the threshold have been suggested – a few per cent of the maximum phase space diameter [13], a value which should not exceed 10% of the mean or the maximum phase space diameter [7,23], or a value that ensures a recurrence point density of approximately 1% [24]. Further suggestions are to choose ε according to the recurrence point density of the RP by seeking a scaling region in the recurrence point density [24] or to take into account that a measurement of a process is a composition of the real signal and some observational noise with standard deviation σ [18]. In order to get similar results as in noise-free situations, ε has to be about five times larger than the standard deviation of the observational noise, i. e. $\varepsilon > 5\,\sigma$. But this approach fails for signals of very low signal-to-noise ratio (SNR) or if the amount of noise is unknown. In any case, the choice of the threshold depends on the aim of the analysis. For example, in a recurrence based synchronisation analysis or for joint recurrence plots (JRPs) [15], the threshold should be chosen in a fashion, that the recurrence point density is the same in the individual RPs.

In the following we will study the impact of recurrence threshold on signal detection [1,21,22]. As a prototypical and analytically well understood example we consider deterministic

[a] e-mail: schinkel@agnld.uni-potsdam.de

signals in a noisy environment (additive noise) and use several recurrence based measures in order to separate a signal from noise. We evaluate the applicability of this procedure in signal detection by *receiver operating characteristics* (ROC) [3,14,25]. To assess our findings in the model system we apply it to electroencephalographic (EEG) data obtained in a classical setup – the oddball paradigm [17].

2 Recurrence based detectors

Deterministic signals have a different recurrence structure than purely stochastic ones. Therefore, it was suggested to apply RQA to distinguish stochastic and deterministic processes [1,14,21,22]. The base of the RQA is the recurrence plot, which visualises recurrences in the phase space of a state vector $\boldsymbol{x}_i$ $(i = 1, \ldots, N)$,

$$R_{i,j} = \Theta(\varepsilon - ||\mathbf{x_i} - \mathbf{x_j}||), \tag{1}$$

where Θ is the Heaviside function, $||\cdot||$ is a norm and ε is the recurrence threshold. For an overview about RPs and related aspects see [11]. RQA provides several measures of complexity. The *recurrence rate RR*

$$RR = \frac{1}{N^2} \sum_{i,j} R_{i,j}, \tag{2}$$

is the density of recurrence points in an RP and can be interpreted as the probability that any state will recur. A phase space trajectory of a deterministic system is characterised by epochs where different segments of this trajectory run parallel for some time. This behaviour is mirrored in the formation of diagonal line structures in the RP.

Denoting the number of lines of exactly length l with $P(l)$, the RQA measure *determinism* DET is defined by

$$DET = \frac{\sum_{l \geq l_{\min}} l\, P(l)}{\sum_l l\, P(l)}, \tag{3}$$

where $l_{\min}$ is the minimal length of a diagonal line necessary to be considered; in the present work we use $l_{\min} = 2$. DET can be interpreted as the probability that two closely evolving segments of the phase space trajectory will remain close for the next time step. Note that *determinism* does not relate to the mathematical notion of the term as such but rather stresses the fact that RPs of stochastic processes usually reveal fewer diagonal lines, whereas RPs of deterministic processes contain more and longer diagonal line structures.

Instead of considering diagonal lines, we can measure vertical recurrence lines and estimate histograms $P(v)$ of vertical line lengths v. The measure

$$LAM = \frac{\sum_{v \geq v_{\min}} l\, P(v)}{\sum_v v\, P(v)}, \tag{4}$$

is called *laminarity* (in the present work we use $v_{\min} = 2$) and measures the probability that a state will not change (within the ε error) for the next time step. Such behaviour is typical for intermittency and laminar states [12].

The last measure considered here is the mean *recurrence time RT*,

$$RT = \frac{\sum_{w=1}^{N} w\, P(w)}{\sum_{w=1}^{N} P(w)}. \tag{5}$$

As an estimator of recurrence time, we measure the vertical distance w between recurrence structures in an RP (corresponding to the length of white vertical lines if $R_{i,j} = 1$ is black and $R_{i,j} = 0$ is white). The number of vertical distances of exact length w is denoted by $P(w)$. Note that this estimator is a lower limit estimator. A definition of an upper limit estimator can be found in [5].

3 Receiver operating characteristic

Signal detection can be considered as a binary classification procedure by using a measure λ, where for $\lambda \geq \eta$ the signal is detected – otherwise not. The *receiver operating characteristic* (ROC) is a plot of the probability to detect the signal correctly with λ (true positives, p_t) vs. the probability to classify the measurement as a signal although it is not (false positives, p_f) [3,25]. In the theory of statistical testing p_t is also referred to as the *power* of a test. As the values of p_t and p_f correspond to the *sensitivity* and $(1 - specificity)$ respectively, for an optimal detection, a high value of p_t and a low value of p_f is desired.

The ROC curve serves as a performance measure of the chosen detector λ. A diagonal line means that classification of the signal or the noise as signal is equiprobable. Therefore, a reliable signal detection is only achieved, if the ROC curve evolves above the diagonal (Fig. 3C).

As a summary of the ROC the area under the curve (AUC) is frequently used. The higher the AUC the better the detector performs. The AUC corresponds to the probability that a signal will have a higher λ than the "no-signal". A value of AUC = 1 corresponds to a 100% correct classification, whereas for AUC = 0.5 we are not able to distinguish signal from noise.

To calculate the ROC we use 10,000 realisations of Gaussian white noise ξ, where we consider a signal s to be modified by additive noise resulting in the measurement $x = s + \xi$. For each realisation we compute the measures RR, DET and RT of the measurement x as well as for the noise ξ, providing the frequency distributions $h_x(\lambda)$ and $h_\xi(\lambda)$ of the values of the detector for the measurement x and the noise ξ (Fig. 3A, B). From the probability distributions $\tilde{h}_x = h_x / \sum h_x$ and $\tilde{h}_\xi = h_\xi / \sum h_\xi$ we calculate the probabilities of true and false positives by

$$p_t = \int_\eta^\infty h_x(\lambda)\, d\lambda \qquad \text{and} \qquad p_f = \int_\eta^\infty h_\xi(\lambda)\, d\lambda. \tag{6}$$

In order to get the ROC curve, p_t and p_f are calculated for $\eta \in [\min(\lambda)\ \ \max(\lambda)]$.

4 Optimal recurrence threshold for a prototypical example

The main purpose of this work is to find a suitable criterion for the selection of an optimal recurrence threshold ε capable of detecting a deterministic signal in a noisy environment. Therefore the threshold with the highest AUC would be optimal for our purpose.

In order to study the AUC for different ε, we use a prototypical example providing a deterministic chaotic signal. We employ the first component of the quasiperiodically forced logistic map [20] as the deterministic signal s

$$s_{i+1} = f \cos(2\pi\theta_i) - a s_i + s_i^3 \tag{7}$$
$$\theta_{i+1} = \theta_i + \omega \bmod 1. \tag{8}$$

For parameters $a = 1.3$ and $f = 0.7$, the system is in a chaotic regime (Fig. 1). For the analysis we used only 600 values (transients at the beginning were removed). The measurement x is formed by the composition of the normalised signal s ($\mu = 0,\ \sigma = 1$) and Gaussian white noise ξ ($\mu = 0,\ \sigma = 1$), i.e. $x = s + a\xi$, where a is the noise level, μ the mean and σ the standard deviation. In this example we use a noise level of $a = 0.75$.

As the map is 2-dimensional the RP is calculated using an embedding dimension of $m = 2$ and a delay of $\tau = 1$. The RP of the signal s clearly reveals diagonal line structures indicating deterministic behaviour (Fig. 2A). These structures persist if the signal is slightly corrupted by noise (Fig. 2C).

For a given recurrence threshold ($\varepsilon = 0.5$), the histograms for the RR measure are presented in Fig. 3A and B. The overlap of the histograms of RR for the noise corrupted signal and the Gaussian white noise is small, providing a good discrimination of the signal. The corresponding ROC confirms the good performance of this measure (Fig. 3C). It should be noted that the distributions of the measures do not follow a normal distribution (gray line in Fig. 3A, B). This is important for the calculation of the ROC, because it can yield different results [9].

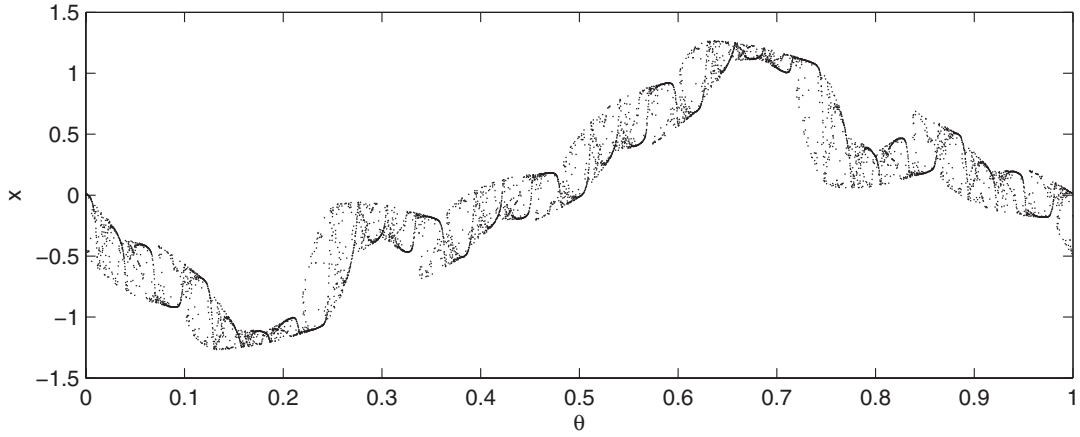

Fig. 1. Quasiperiodically forced logistic map.

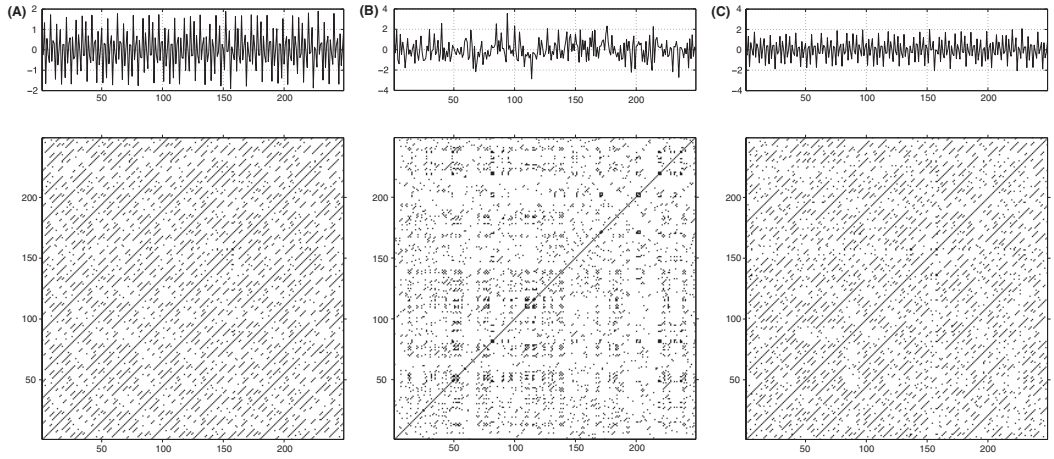

Fig. 2. Detail of the recurrence plot of (A) the quasiperiodically forced logistic map, (B) Gaussian white noise and (C) a noise corrupted signal of the quasiperiodically forced logistic map (noise level 0.1). Embedding parameters $m = 2$, $\tau = 1$, recurrence threshold $\varepsilon = 0.5$.

We calculate the AUC for the measures RR, DET, LAM and RT with varying $\varepsilon \in [0\,1.5]$. If ε is too small, recurrences mainly appear due to the fluctuations caused by the noise. A discrimination of the signal is therefore difficult and the AUC is low (Fig. 4). For increasing ε the RP obtains the recurrence structure contained in the signal. The detection of the signal becomes better and the AUC is high. If ε becomes too large almost every point is in the neighbourhood of every other point, thus hiding the characteristic recurrence structure. The signal is again not well detectable and the AUC is decreasing. Such a behaviour can be observed in RR, DET and RT (Fig. 4). The measures RR and DET perform best with a maximum AUC of about .8 (RR) or even .9 (DET) for $\varepsilon = 0.4$. In contrast, the AUC for RT is significantly smaller and has its maximum of 0.6 for $\varepsilon = 0.15$. This suggests that RT is not an optimal detector for chaotic maps. The measure LAM shows a completely different behaviour. Its values are below 0.5, indicating that LAM falsely classifies noise as the signal. That is due to the fact the RP of noise contains more vertical structures than the RP of the signal (Fig. 2) which does not contain any laminar phases. Therefore, the measure LAM is not appropriate for detecting a deterministic signal as considered here. However, as we will see later, this measure is a useful detector for signals like EEGs which do contain laminar phases.

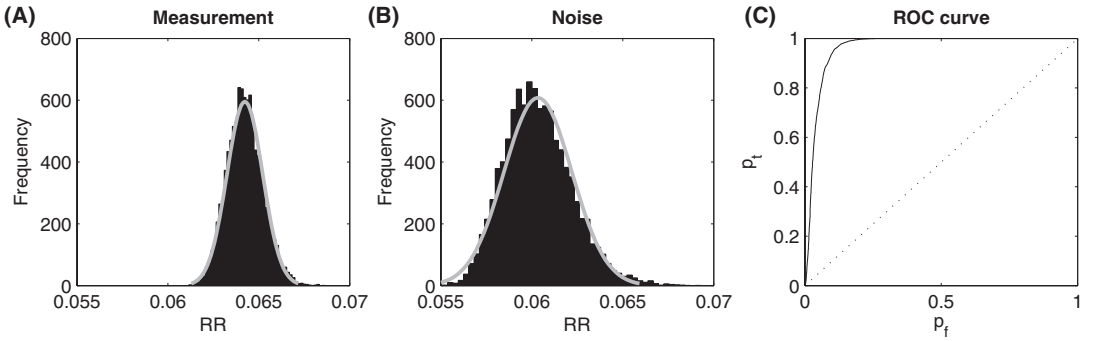

Fig. 3. Histogram of the RR detector for 10,000 realisations of a measurement containing (A) a signal from the quasiperiodically forced logistic map and (B) Gaussian white noise. A fit of a normal distribution is presented as a gray line. By applying a threshold on the detector RR we will be able to detect the signal in most cases. This is characterised by (C) the ROC curve, which is based on the probabilities to detect true positives (p_t) and false positives (p_f). If the ROC curve would follow the diagonal line (dotted line), we would not be able to distinguish the signal from noise.

5 Application to EEG measurements

We apply the suggested procedure to EEG measurements of a study on event-related potentials (ERPs). The paradigm used was a visual *oddball* featuring a prominent P300, which is a centro-parietal positivity peaking at about 300 ms after the presentation of a stimulus. The P300 has been shown to be senstive to stimulus category (target vs. non-target) of the eliciting stimulus [17].

The simuli were red and green disks presented in randomised, equiprobable order. Stimulation duration was 100 ms, the interval between successive stimuli 900 ms. The task was to count the items of one colour (green or red) thereby constituting the target (A) (items to be counted) and non-target condition (B). This setup is known to elicit a prominent and reproducible P300 in the target condition (compared to the non-target condition).

The EEG was recorded from 40 Ag/AgCl electrodes (impedances $\leq 5\,\mathrm{k}\Omega$) at a sampling rate of 250 Hz using a BrainAmp DC amplifier (Brain Products GmbH, Munich, Germany). All electrodes were initially referenced to an electrode on the left mastoid bone (A1) and converted to average reference off-line. After standard artifact rejection about 250 trials remained in each condition. For our purpose we selected 200 trials of one subject recorded at electrode PZ. The data was baseline corrected to 100 ms pre-stimulus. Details of artifact rejection and pre-processing can be found in [26].

We consider a pre-stimulus interval of 250 ms duration, immediately before the stimulus (−200–50 ms) and a 250 ms interval during the P300 (200–450 ms). During the pre-stimulus, the two measurements of condition A and B should not be distinct, resulting in a AUC of around 0.5. In contrast, if the detectors are able to distinguish the two conditions, their AUC values should be higher than 0.5. For the computation of the ROC the 200 trials are used as realisations. The AUCs are calculated for recurrence thresholds ε between 0.1 and 1.0 with steps of 0.01, and using an embedding of $m = 3$ and $\tau = 2$. The embedding parameters were estimated using the commonly accepted methods of false nearest neighbours and mutual information [6].

As expected, the AUCs for all detectors in the pre-stimulus interval are around 0.5, indicating that there is no difference between the measurements before the onset of the stimulus (Fig. 6). Only LAM and RT reveal slightly smaller or higher values for ε between 0.1 and 0.2.

During the occurrence of the P300, the AUCs for the detectors RR, DET, and LAM are higher than 0.5, indicating that these measures are able to discriminate between condition A and B. However, the highest AUC value is 0.61 for RR and LAM, and 0.63 for DET, which is not really high. The RT is not a good detector as it again fails in discriminating the two

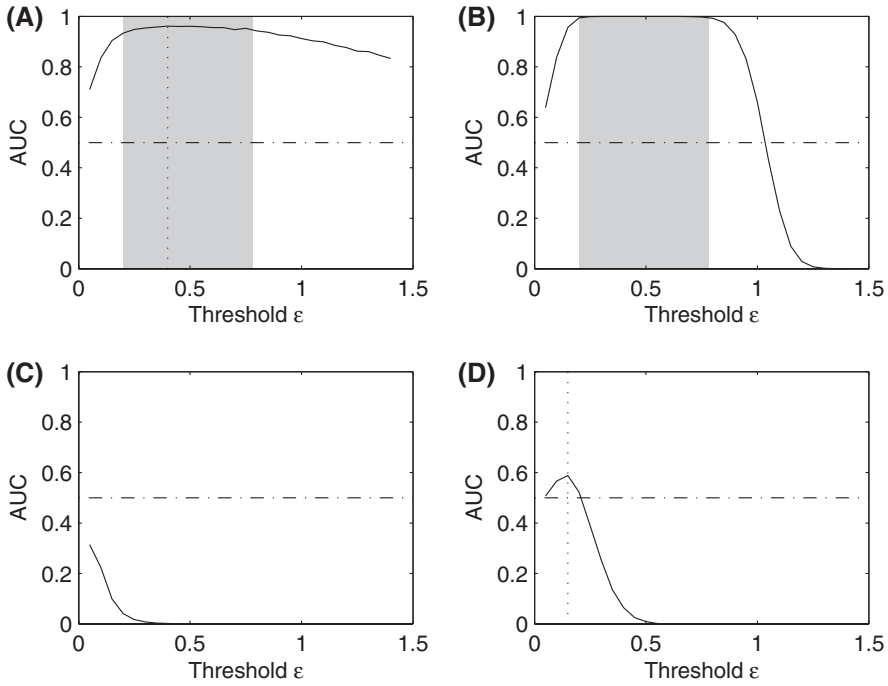

Fig. 4. AUCs vs. ε for the measures (A) RR, (B) DET, (C) LAM and (D) RT for the quasiperiodically forced logistic map. The AUC for RR and DET (A, B) is rather high in a range of $\varepsilon \in [0.2\,0.78]$, with the maximum at $\varepsilon = 0.4$ (dotted line). The AUC of RT (D) is significantly lower, with a maximum at $\varepsilon = 0.15$ (dotted line). The AUC of LAM is lower than 0.5, indicating that this measure falsely classifies noise as signal. An AUC level of 0.5 (dash-dotted line) means that the detector is not able to find the signal.

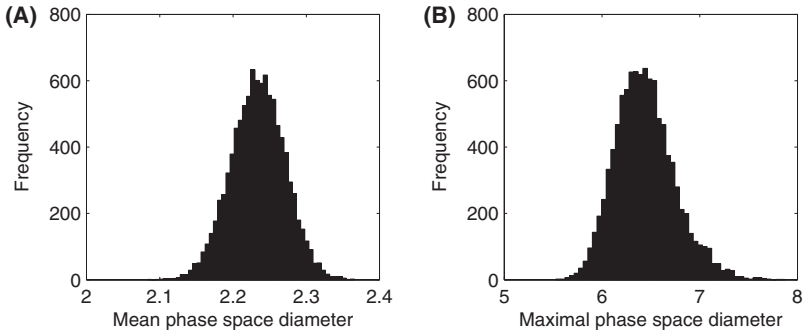

Fig. 5. Distribution of (A) mean and (B) maximal phase space diameter of 10,000 realisations of the noise corrupted quasiperiodically forced logistic map in an embedding space of $m = 2$ and $\tau = 1$.

conditions. As we found in previous works, other RQA measures (like *trapping time*) [10] or the application of *order pattern recurrence plots* [8,16] reveal better results. Nevertheless, we find the optimal recurrence threshold as $\varepsilon = 0.25$, for RR and LAM, or as $\varepsilon = 0.22$, for DET. The mean and maximal phase space diameter for the pre-stimulus and the P300 epochs of the ERP data of both conditions are 2.40 and 5.55, respectively. Thus, the optimal $\varepsilon = 0.25$ found corresponds to 10% of the mean and 5% of the maximal phase space diameter. Regarding the standard deviation $\sigma(x) = 1$ of the ERP signal itself, ε is 25% of the standard deviation.

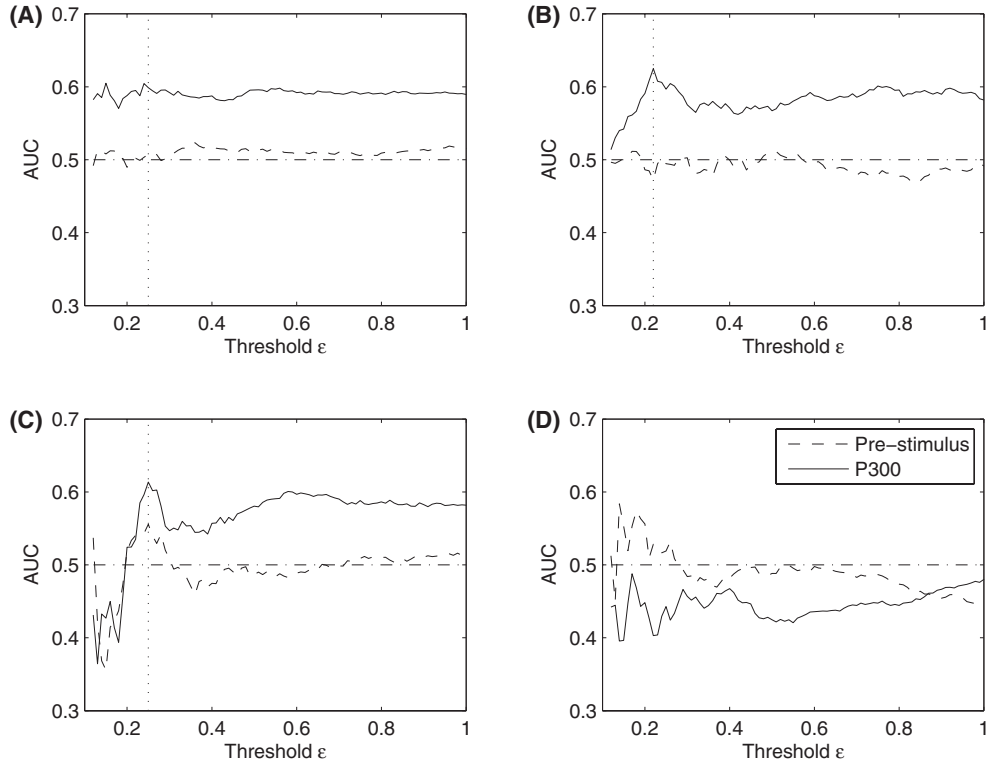

Fig. 6. AUCs vs. ε for the measures (A) RR, (B) DET, (C) LAM and (D) RT for ERP data on a pre-stimulus period (dashed line) and during the P300 event (line). AUC maxima for RR and LAM at $\varepsilon = 0.25$, and for DET at $\varepsilon = 0.22$ (dotted line). An AUC level of 0.5 (dash-dotted line) means that the detector is not able to find the signal. Embedding parameters are $m = 3$ and $\tau = 2$.

In contrast to the prototypical example of the quasiperiodically forced logistic map discussed above, the ERP signal contains laminar states at the P300. Therefore, LAM now is a suitable detector for the P300.

6 Discussion

The search for a recurrence threshold for an optimal discrimination of signals has revealed different optimal thresholds ε depending on the application and considered type of signal (Tab. 1). Using the recurrence probability alone for the detection may require another threshold than using diagonal and vertical line structures. However, the differences in the optimal ε are not big, and of course the optimal threshold also depends on the amount of noise present in the measurement.

For the quasiperiodically forced logistic map the threshold $\varepsilon = 0.4$ at the maximum of AUC corresponds to a calculated RR of the system of 4%. This suggests that the threshold should be chosen in such a way that the RR would be around 5%. Several authors suggested values of ε relative to the mean and maximal phase space diameter [7,23]. The mean phase space diameter

Table 1. Optimal recurrence thresholds ε and corresponding percentages of mean and maximal phase space diameter (mean PSD and max. PSD) as well as signal standard deviation σ.

	ε	mean PSD	max. PSD	σ
quasiperiodically forced logistic map	0.4	18%	6%	40%
ERP data	0.25	10%	5%	25%

of the noise corrupted quasiperiodically forced logistic map (normalised to standard deviation one) is 2.23 and its maximal diameter is 6.43 (Fig. 5). Therefore $\varepsilon = 0.4$ corresponds to 18% of the mean and 6% of the maximal phase space diameter respectively. As our aim here is an appropriate classification of signal and noise and not the detection of the original recurrence structure, choosing $\varepsilon > 5\,\sigma$, as suggested for the case of observational noise [18], is not beneficial here. Considering the noise level of $a = 0.7$, $5\,\sigma(\xi)$ would result in a value of 2.5 for ε. Indeed, this value is too high to correctly classify signal and noise. Compared to the standard deviation of the entire, normalised signal $\sigma(x) = 1$, ε equals 40% of $\sigma(\xi)$.

For the experimental data, we found that the optimal threshold is 10% of the mean phase space diameter or 25% of the standard deviation. For the prototypical example, where the influence of noise is far smaller than in the experimental data, we found a threshold almost twice as large, given as 18% of the mean phase space diameter and 40% of the standard deviation. The most consistent choice would be regarding the maximal phase space diameter, where we found values of around 5–6% of the maximal phase space diameter in both experiments.

Although only demonstrated using two examples and knowing well that the matter needs to be investigated more comprehensively, our study confirms the suggested rule of thumb that the threshold should be around 5% of the maximal phase space diameter. This suggestion remained valid for two very different kinds of signal of different complexity, a priori knowledge and noise influence. Hence it seems to be rather robust, at least for the purpose of signal detection.

7 Conclusions

We have proposed a new approach for the choice of an optimal recurrence threshold ε for the classification of signals. Our method uses the notion of *receiver operating characteristics* (ROC), a statistical tool to validate a classification process and investigate its discriminative power in dependence of a given detector, in the present case the complexity measures as derived from an RP using the RQA. We could demonstrate the discrimination of (i) signals from pure noise and (ii) of different experimental conditions given as extremely noisy and instationary time series typical for EEG measurements. Our results support the proposed rule of thumb, that the recurrence threshold ε for optimal signal classification/discrimination should be about 5% of the maximal phase space diameter.

This work was supported by grants of the European Union through the Network of Excellence BioSim, contract LSHB-CT-2004-005137 & No. 65533, the German Science Foundation (DFG) in the SFB 555 *Komplexe nichtlineare Systeme* and the Research Group FOR 868: *Computational Modeling of Behavioral, Cognitive and Neural Dynamics*, and the COST Action BM0601 *NeuroMath: Advanced Methods For The Estimation Of Human Brain Activity And Connectivity*. The software (CRP Toolbox) used for this work is partly available for download at http://tocsy.agnld.uni-potsdam.de.

References

1. T. Aparicio, E.F. Pozo, D. Saura, J. Econom. Behav. Org. **65**, 768 (2008)
2. L. Cao, Physica D **110**, 43 (1997)
3. T. Fawcett, Patt. Recogn. Lett. **27**, 861 (2006)
4. A.M. Fraser, H.L. Swinney, Phys. Rev. A **33**, 1134 (1986)
5. J.B. Gao, H.Q. Cai, Phys. Lett. A **270**, 75 (2000)
6. H. Kantz, T. Schreiber, *Nonlinear Time Series Analysis* (University Press, Cambridge, 1997)
7. M. Koebbe, G. Mayer-Kress, *Proceedings of SFI Studies in the Science of Complexity*, edited by M. Casdagli, S. Eubank, Vol. 21 (Redwood City, Addison-Wesley, 1992), p. 361
8. N. Marwan, A. Groth, J. Kurths, Chaos Complex. Lett. **2**, 301 (2007)
9. N. Marwan, J. Kurths, Rohde et al., Physica D **237**, 619 (2008); Physica D (submitted)
10. N. Marwan, A. Meinke, Int. J. Bifurc. Chaos **14**, 761 (2004)
11. N. Marwan, M.C. Romano, M. Thiel, J. Kurths, Phys. Rep. **438**, 237 (2007)
12. N. Marwan, N. Wessel, U. Meyerfeldt, A. Schirdewan, J. Kurths, Phys. Rev. E **66**, 026702 (2002)

13. G.M. Mindlin, R. Gilmore, Physica D **58**, 229 (1992)
14. G.K. Rohde, J.M. Nichols, B.M. Dissinger, F. Bucholtz, Physica D **237**, 619 (2008)
15. M.C. Romano, M. Thiel, J. Kurths, I.Z. Kiss, J. Hudson, Europhys. Lett. **71**, 466 (2005)
16. S. Schinkel, N. Marwan, J. Kurths, Cognit. Neurodyn. **1**, 317 (2007)
17. S. Sutton, M. Braren, J. Zubin, E.R. John, Science **150**, 1187 (1965)
18. M. Thiel, M.C. Romano, J. Kurths, R. Meucci, E. Allaria, F.T. Arecchi, Physica D **171**, 138 (2002)
19. A.A. Tsonis, Int. J. Bifurc. Chaos **17**, 4229 (2007)
20. A. Venkatesan, M. Lakshmanan, Phys. Rev. E **63**, 026219 (2001)
21. J.P. Zbilut, A. Giuliani, C.L. Webber Jr., Phys. Lett. A **267**, 1742 (2000)
22. J.P. Zbilut, A. Giuliani, C.L. Webber Jr., Phys. Lett. A **246**, 122 (1998)
23. J.P. Zbilut, C.L. Webber Jr., Phys. Lett. A **171**, 199 (1992)
24. J.P. Zbilut, J.-M. Zaldívar-Comenges, F. Strozzi, Phys. Lett. A **297**, 173 (2002)
25. M.H. Zweig, G. Campbell, Clin. Chem. **39**, 561 (1993)
26. M. Valsecchi, O. Dimigen, R. Kliegl, W. Sommer, M. Turratto (accepted)